Available online at www.sciencedirect.com
ScienceDirect
Journal of Non-Crystalline Solids 352 (2006) 3550–3555
JOURNAL OF NON-CRYSTALLINE SOLIDS
www.elsevier.com/locate/jnoncrysol

Effect of temperature on hardness and indentation cracking of fused silica

M.D. Michel [a,b], F.C. Serbena [a,*], C.M. Lepienski [b]

[a] Departamento de Física, Universidade Estadual de Ponta Grossa, av. Carlos Cavalcanti, 4748, Ponta Grossa, PR 84030-900, Brazil
[b] Departamento de Física, Universidade Federal do Paraná, Centro Politécnico, Cx. Postal 19044, Curitiba, PR 81531-990, Brazil

Available online 24 July 2006

Abstract

The fracture behavior induced by Vickers indentations in fused silica was investigated as a function of temperature. Indentations were performed from room temperature to 400 °C in air. The indentations and the crack pattern formed were analyzed by optical and scanning electron microscopy. The hardness at room temperature was 7.3 ± 0.3 GPa and decreased to 4.2 ± 0.1 GPa at 400 °C. Cone and radial cracks were observed at all temperatures. The radial crack length increased with temperature for a constant load. Lateral and median cracks were present under the indenter, and their expansion was constrained by cone cracks nucleated during the loading-unloading cycle. The threshold loads for cone and radial crack nucleation increased with temperature. The results are discussed in terms of the elastic modulus/hardness ratio variation with temperature.

PACS: 81.05.Kf; 62.20.Mk; 62.20.Qp

Keywords: Mechanical properties; Fracture; Indentation, microindentation; Silica

1. Introduction

Silica is a material used in many industries as in communications and optics. It is also one of the main constitutions of other glasses, used in automotive, architecture, insulation, bottle and reinforcement industries.

Silica glasses with about 30% of other oxides, like soda–lime glass (SLS), show the usual radial, median and lateral crack system when indented. However, if the silica content is much higher, densification occurs in the volume beneath the indenter and cone cracks are nucleated [1,2].

Cook and Pharr investigated experimentally the crack nucleation of several transparent brittle materials during Vickers indentation at room temperature [3]. They used an inverted optical microscope under the sample in an instrumented indenter and observed in situ the different cracks that appeared during the indentation process. They proposed a model that showed that the sequence of appearance of the different cracks along the loading/unloading curve is strongly influenced by the material parameter fE/H, where f is a constant related to densification that occurs in anomalous glasses, E is the elastic modulus and H is the material hardness.

Usually E decreases by a small amount compared to H as temperature increases. Therefore, fE/H increases as the temperature raises and there should be a change in the crack nucleation sequence according to the Cook and Pharr analysis. In a previous paper, the fracture modification with temperature was analyzed for SLS glass [4]. It was verified a dependence of crack nucleation with temperature.

There have been a few papers that studied the effect of temperature on deformation of fused silica [5,6]. The purpose of this article is to investigate the hardness and crack behavior of fused silica as a function of temperature. In a previous paper [4], the effect of temperature

* Corresponding author. Tel.: +55 42 220 3044; fax: +55 42 220 3042.
E-mail address: fserbena@uepg.br (F.C. Serbena).

0022-3093/$ - see front matter © 2006 Elsevier B.V. All rights reserved.
doi:10.1016/j.jnoncrysol.2006.02.113

was investigated in commercial soda-lime silica glass, which does not densify. The crack morphology is described as a function of temperature and is analyzed by optical and scanning electron microscopies (SEM).

2. Experimental procedure

Commercial fused silica specimens in the form of rectangular bars with dimensions of $3 \times 8 \times 25$ mm were used. The samples presented a good surface finishing. They were immersed in distilled water for 24 h in order to develop all surface microcracks and dried at room temperature in air. Samples were annealled at 840 °C (±10 °C) for 1 h in air to relieve the residual stresses and cooled inside the furnace at a rate of ≈5 °C/min.

Vickers indentations at high temperatures were performed by an apparatus described previously [4]. Indentations from 0.5 to 40 N at 20 °C to 400 °C with a dwell time of 60 s in air were performed. At least 4 indentations were performed for each load. A film of silicon oil was applied over the surface prior to indentation at room temperature and 200 °C to minimize the post-indentation environmentally assisted crack growth due to air humidity. At 400 °C, the indentations were made without silicon oil applied. During cooling, when the temperature of 200 °C was reached, a few drops of silicon oil pre-heated at 200 °C (to avoid thermal shock which could promote crack growth) was dropped over the surface and the specimen was allow to cool to room temperature.

The Vickers hardness H was calculated according to [7]:

$$H = 1.854\frac{P}{d^2}, \quad (1)$$

where P is the load and d is the average of the impression diagonals.

The samples were immediately observed afterwards by optical microscopy. Some samples were also observed by SEM. Some of them were also sectioned transversely in a bending apparatus for a better observation of the crack morphology beneath the indenter. In this case, only one indentation was made in the center of the sample. During bending, the radial cracks propagated to fracture the sample showing the cross section of the indented area.

Some additional experiments were performed at room temperature to determine the threshold loads for radial and cone cracks. Silicon oil was dropped into the surface to avoid the effect of air moisture in these experiments.

3. Results

Fig. 1 shows the decrease in hardness with temperature for fused silica. It decreases from 7.3 ± 0.3 GPa at room temperature to 4.2 ± 0.1 GPa at 400 °C. The load used for measuring hardness was 5 N for 200 °C and 400 °C. A well defined impression was obtained similar as seen in Fig. 2(b) for this load at 400 °C. At 200 °C, it was observed cracking around and at the Vickers impressions. In some of them, the cracking was so severe that the diagonals were damaged and no measurement was possible. Therefore, a larger number of indentations were performed at this temperature to allow for hardness measurements. At room temperature, it was observed severe cracking at and around the impressions for a load of 5 N as seen in Fig. 2(a), and it was complete unsuitable measuring the diagonals. Therefore, a load of 1 N was used to obtain impressions with well defined diagonals.

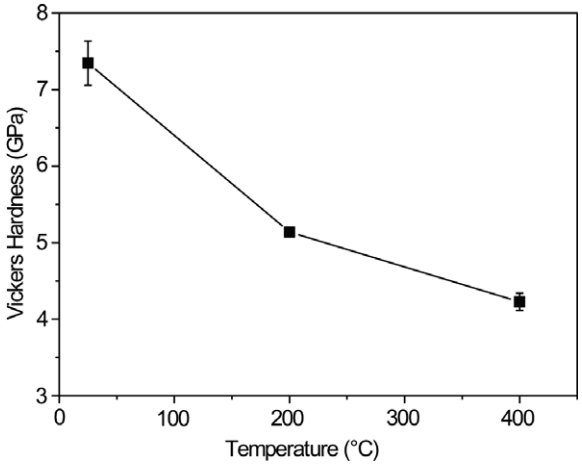

Fig. 1. Variation of Vickers hardness with temperature. The loads used were 1 N for room temperature and 5 N at 200 °C and 400 °C. The lines are a guide to the eye only.

The cracks around the impressions at 20 °C and 400 °C are shown in Figs. 2 and 3 for applied loads of 5 N and 40 N. Cone cracks are present for all loads at room temperatures. Lateral and radial cracks are also observed. Median cracks are recognized under the plastic zone at 40 N. At room temperature, there are a significant number of secondary radial cracks (cracks that are not aligned with the impression diagonals). Also observed in Fig. 3(a) and (c) is that radial cracks do not have the familiar semicircular or Palmqvist forms. Their expansion is confined by the cone crack, indicating cone cracks are nucleated before the radials. Only radial and lateral cracks are observed for 5 N at 400 °C as observed in Fig. 3(b). Also, the radial cracks at this temperature are mainly primary (aligned along the diagonals impressions) and are longer than at room temperature as seen in Fig. 2(c) and (d). At 400 °C, there is a great reduction in the number of secondary radial cracks. One can be seen at the lower corner of the impression in Fig. 2(b). The median crack created at 40 N is longer at 400 °C than at 20 °C as observed in Fig. 3(c) and (d).

Fig. 4 shows the radial crack length as a function of the applied load at different temperatures. The crack length increases with temperature. At 5 N, the crack increases from about 33 ± 7 μm at 20 °C to 51 ± 15 μm at 400 °C. This is an increase of 55% approximately. This relative increase is 65%, 64% and 23% for the loads of 10 N, 20 N and 40 N, respectively. It was pointed out by Anstis

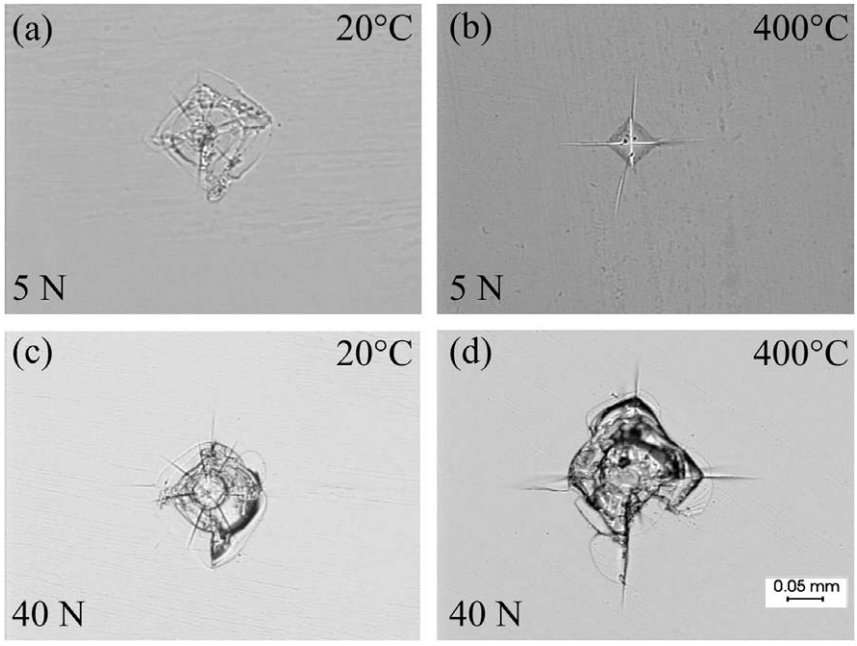

Fig. 2. Optical micrographs of indentations performed at (a) 5 N and 20 °C, (b) 5 N and 400 °C, (c) 40 N and 20 °C and (d) 40 N and 400 °C. The scale is the same for all figures.

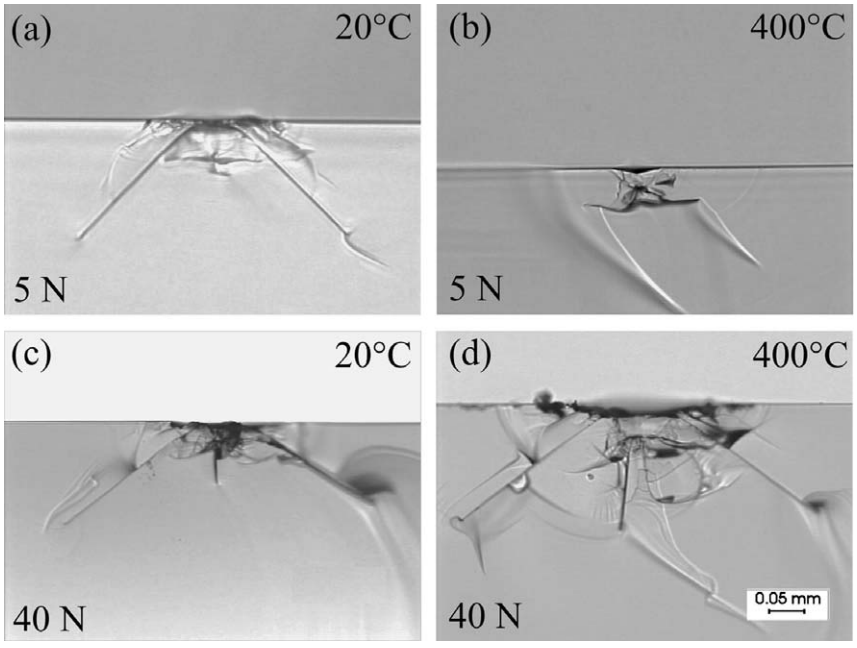

Fig. 3. Optical micrographs of cross section of the same indentations shown in Fig. 2 performed at (a) 5 N and 20 °C, (b) 5 N and 400 °C, (c) 40 N and 20 °C and (d) 40 N and 400 °C. The scale is the same for all figures.

et al. [8] that the radial crack length c is related on load P according to:

$$P = k^{-1}\left(\frac{H}{E}\right)^{1/2} K_C \cdot c^{3/2} \quad (2)$$

where K_C is the fracture toughness and k is a constant that depends on indenter geometry and is equal to 0.016 ± 0.004. Fig. 5 shows the plot of P against $c^{3/2}$. Eq. (2) is well obeyed at 20 °C and 200 °C and reasonably at 400 °C. From Eq. (2), fracture toughness can be evaluated. Assuming E as equal to 72 GPa [3], a K_C value of 1.3 ± 0.4 MPa $m^{1/2}$ with a correlation factor of 0.99926 was obtained from the least square fitting of the crack length and load data at room temperature of Fig. 5.

At 400 °C, the threshold load for radial crack nucleation is below 4.2 N as seen in Fig. 6. The edges of lateral cracks

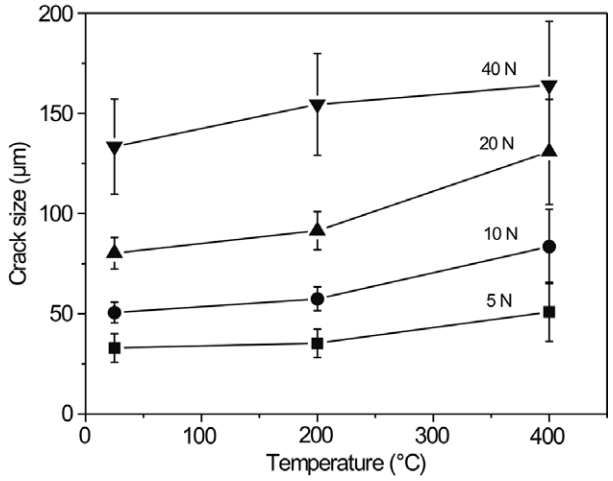

Fig. 4. Variation of radial crack size with temperature for different loads. The lines are a guide to the eye only.

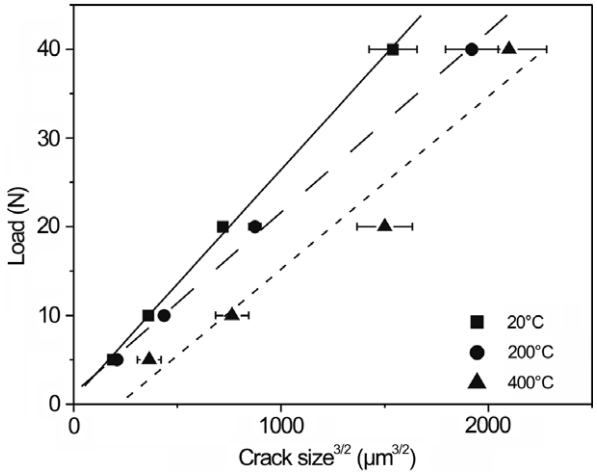

Fig. 5. Crack size variation as a function of load at different temperatures. The lines are a least mean square fitting of the data.

are seen fainted in the micrographs, but no cone cracks are visible. Some experiments were performed for determination of the threshold load for cone cracks nucleation. This was found to be around 6 N at 400 °C. In Fig. 7(a), it is seen a partially nucleated lateral crack and in Fig. 7(a) and (b) cone crack. Additionally, it was found the radial cracks are nucleated at loads as low as 0.5 N and cone cracks begin to nucleate at loads between 2 and 5 N at room temperature.

The main factor believed to affect the results is the mechano-chemical effect due to air moisture. A film of silicon oil was used to attenuate this effect. However, we cannot rule out a small increase in crack length due to this effect. Also, there is a time interval between the first and the last indentation of a test. Therefore, the first indentation is more affected by environmentally assisted crack growth due to air humidity than the last one. The time for sample observations under a microscope also assisted this effect. Another factor that might have influenced the results was that the time for microscope analysis was shorter for tests at room temperature than for those at higher temperature after the tests due to the time for sample cooling.

4. Discussion

Hardness of fused silica measured at room temperature is in accordance with values obtained by other authors [2,3,9,10]. Increasing the temperature to 400 °C, hardness decreases to a value that is about 60% the room temperature value, which is the same amount as observed previously for SLS glass indented under similar conditions [4]. Beake and Smith [6] measured the hardness dependence with temperature in fused silica using an instrumented indentation. They observed a decrease in hardness from 8.9 to 8.4 GPa when indenting from room temperature to 400 °C. This is a much smaller decrease then observed in this work. This might be due to the lower loads used in their work (0.2 N) and the shorter dwell time (10 s).

Cook and Pharr [3] observed that cone cracks were nucleated at the beginning of the loading cycle in fused silica at room temperature. Further during the loading cycle, primary radial cracks appeared and subsequently secondary radials. Lateral cracks appeared during the unloading cycle followed by another group of secondary radials. This is in accordance with what is observed in Fig. 3(a), (c) and (d).

One feature observed in Figs. 2 and 3 is the nucleation of cone cracks at room temperature but not at 400 °C for an applied load of 5 N. In fact, the indentation cracking shown in Figs. 2(b) and 3(b) resembles an indentation of materials like SLS glass. Cone cracks are typical for high content silica glass while they are not observed in SLS

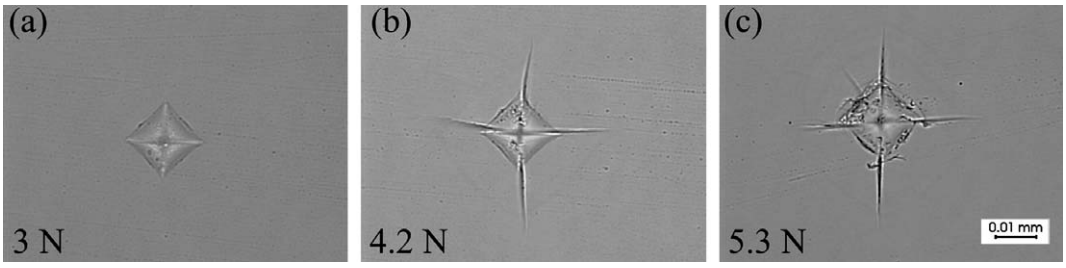

Fig. 6. Optical micrographs of Vickers indentations at 400 °C for a load of (a) 3 N, (b) 4.2 N and (c) 5.3 N showing nucleation of only radial cracks, but not of cone cracks. The scale is the same for the figures.

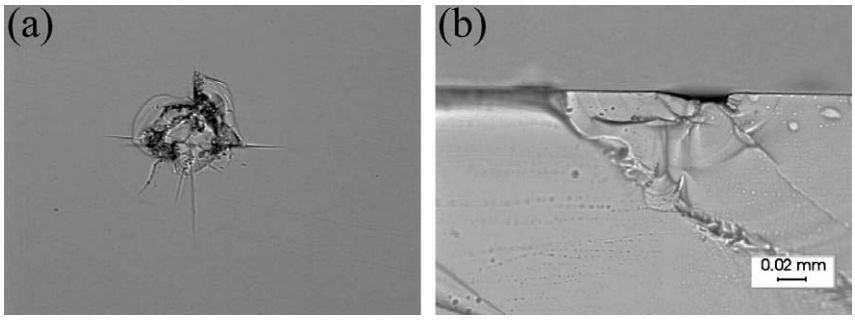

Fig. 7. Optical micrographs of (a) top view and (b) side view of a Vickers indentation performed at 400 °C and load of 7.3 N showing the partial nucleation of cone cracks. The scale is the same for all figures.

glasses at room temperature [2,4]. Primary radial cracks are nucleated at the beginning of the unloading cycle and lateral cracks at the end [3]. Kurkjian et al. [9] observed ring cracks around Vickers indentation in SLS glass at −196 °C. Cook and Pharr [3] studied the nucleation of different indentation cracks in several materials, including cone and radial cracks. They rationalized that the intensity of the different stress components produced by an expanding cavity [11] depends on the parameter fE/H. By applying their model, they were able to describe qualitatively the sequence of nucleation of different cracks as a function of the fE/H ratio. By decreasing fE/H, there is a tendency for nucleation of cone cracks during loading and a change of nucleation of radial cracks from the unloading towards the loading part of the cycle.

Values of fE/H for fused silica and SLS glass increases as the temperature raises as observed in Table 1. Assuming that the parameter fE/H controls the crack nucleation sequence, it is expected that cracking of fused silica at 400 °C will be similar to SLS glass at room temperature and that SLS glass at −196 °C will be similar to fused silica at room temperature. Partial ring cracks, which appear beforehand cone cracks, are seen in SLS glass at −196 °C [9]. However cone cracks are seen at 400 °C in silica glass but not in SLS glass at room temperature. It has been suggested that this is caused by the compaction of SLS glass at −196 °C [9].

Fig. 4 showed an increase in radial crack length with temperature. This was already been observed for single crystals of Si and SiC [12], MgO [13], ytria-stabilized zirconia [14] and SLS glass [4]. According to Eq. (2), c should increase proportionally to $(E/H)^{1/3}K_C^{-2/3}$ for a constant load. It is observed experimentally that E and K_C do not vary significantly with temperature, while H does. Therefore, increasing the temperature results in a decrease of H and an increase in the factor $(E/H)^{1/3}K_C^{-2/3}$. Consequently, the crack length should increase with increasing temperature.

A K_C value of 1.3 ± 0.4 MPa m$^{1/2}$ was obtained at room temperature. This is ~65% higher than K_{IC} of 0.79 MPa m$^{1/2}$ measured using chevron-notched short rod specimens [15]. Dériano and co-workers [16] measured indentation fracture toughness in silica-rich glasses. They also observed an overestimation of indentation fracture toughness for these glasses. They suggested that the occurrence of flow-densification in the plastic zone relieved the residual stress in the area surrounding the indentation, causing the reduction in the length of radial cracks. Therefore, although Eq. (2) is correct concerning the linearity of P and $c^{3/2}$, the constant 0.016 should be lower for anomalous glasses as silica, borosilicate and silica-rich glasses where densification occurs. Probably, apart from the densification process that relieves partially the stresses of the deformed zone underneath the indenter, there is also the nucleation of cone cracks before the radial cracks which also contributes to the relief of the stresses that drive radial crack propagation.

Threshold loads for radial and cone crack nucleation at 400 °C were about 4 N and 6 N, respectively, which are higher than those measured at room temperature. Lawn and Evans [18] proposed the critical load for median/radial crack nucleation was proportional to K_C^4/H^3. Since H decreases with temperature it is expected an increase in the threshold load. It is also observed in this work that the critical load for nucleation of radial cracks is lower than for cone cracks at 400 °C. This may be caused by the increase of fE/H with temperature, which would (a) make more difficult the nucleation of cone cracks by decreasing the stress component responsible for ring crack nucleation and (b) changes the nucleation of radial cracks towards the unloading [3].

Table 1
Comparison of the parameter fE/H for fused silica and SLS glass

Material	T (°C)	E (GPa)	H (GPa)	fE/H
Fused silica	20	70 [6]	7.3 ± 0.3	8.2 ± 0.3
	400	78 [6]	4.2 ± 0.1	18.6 ± 0.4
SLS glass	−196	75 [17]	11.2 ± 1 [9]	6.7 ± 0.6
	20	73 [17]	5.5 [9]	13.3

It is assumed f is 0.85 for fused silica and 1 for SLS glass [3].

5. Conclusion

Vickers indentations in fused silica revealed a decreased in hardness from 7.3 GPa at room temperature to 4.1 GPa at 400 °C. Cone, radial, lateral and median cracks were

observed at all temperatures. The increase of the radial crack length with temperature follows a relation $c^{3/2}$ proportional to P for all temperatures. The threshold loads for radial and cone cracks nucleation increased with temperature.

Acknowledgment

The authors are grateful to CAPES, CNPq and Universidade Estadual de Ponta Grossa (Brazil) for partial financial support of this work.

References

[1] P.W. Bridgman, I. Simon, J. Appl. Phys. 24 (1953) 405.
[2] A. Arora, D.B. Marshall, B. Lawn, M.V. Swain, J. Non-Cryst. Solids 31 (1979) 415.
[3] R.F. Cook, G.M. Pharr, J. Am. Ceram. Soc. 73 (1990) 787.
[4] M.D. Michel, A. Mikowski, C.M. Lepienski, C.E. Foerster, F.C. Serbena, J. Non-Cryst. Solids 348 (2004) 131.
[5] J.H. Westbrook, Phys. Chem. Glasses 1 (1960) 32.
[6] B.D. Beake, J.F. Smith, Philos. Mag. A 82 (2002) 2179.
[7] P.J. Blau, Metallography 16 (1983) 1.
[8] G.R. Anstis, P. Chantikul, B.R. Lawn, D.B. Marshall, J. Am. Ceram. Soc. 64 (1981) 539.
[9] C.R. Kurkjian, G.W. Kammlott, M.M. Chaudhri, J. Am. Ceram. Soc. 78 (1995) 737.
[10] N. Gougeon, J.C. Sangleboeuf, R.E. Abdi, M. Poulain, C. Tistere-Borda, Fiber Integr. Opt. 24 (2005) 491.
[11] E.H. Yoffe, Philos. Mag. A 46 (1982) 617.
[12] M.G.S. Taylor, T.F. Page, J. Microsc. – Oxford 130 (1983) 345.
[13] N. Khasgiwale, H.M. Chan, J. Am. Ceram. Soc. 75 (1992) 1924.
[14] G.N. Morscher, P. Pirouz, A.H. Heuer, J. Am. Ceram. Soc. 74 (1991) 491.
[15] J.P. Lucas, Scripta Metall. 32 (1995) 743.
[16] S. Dériano, A. Jarry, T. Rouxel, J.C. Sangleboeuf, S. Hampshire, J. Non-Cryst. Solids 344 (2004) 44.
[17] T. Rouxel, J. Sangleboeuf, J. Non-Cryst. Solids 271 (2000) 224.
[18] B.R. Lawn, A.G. Evans, J. Mater. Sci. 12 (1977) 2195.